Journal of Machine Construction and Maintenance
QUARTERLY 1/2018(108)
ISSN 1232-9312
p. 45–52

Daniel GROCHAŁA, Stefan BERCZYŃSKI
West Pomeranian University of Technology Szczecin, Poland
Faculty Mechanical Engineering and Mechatronics
daniel.grochala@zut.edu.pl; stefan.berczynski@zut.edu.pl

Zenon GRZĄDZIEL
Maritime University of Szczecin, Poland
Faculty of Marine Engineering
z.grzadziel@am.szczecin.pl

TESTING OF THE STATE OF STRESSES AFTER FINISH BURNISHING ITEMS

Key words: FEM modelling, residual stresses, plastic surface treatment, burnishing, surface geometric structure, roughness.

Abstract: The article presents the results of studies on the formation of residual stresses due to finish burnishing. Improper state of stresses may arise when, seeking higher dimension and shape accuracy, smaller roughness, or improved plateau area, the production engineer is willing to apply high and very high burnishing forces F_b. Plastic deformations in roughness created by burnishing can be easily measured with modern profilometers. However, each finish burnishing cut is accompanied by a state of stresses, some of which are residual stresses that remain in the item after machining. Excessively high stresses during the use of products are often causes of the cracking and flaking of surface fragments [1, 2]. One of most accurate methods for the evaluation of residual stresses after burnishing is their modelling taking into account the mechanical properties of material and technological parameter values used in the course of machining. The authors discuss the method of developing an experimental model, its testing, and verification of the results.

Badania stanu naprężeń przedmiotów nagniatanych gładkościowo

Słowa kluczowe: modelowanie MES, naprężenia trwałe, plastyczna obróbka powierzchni, nagniatanie, struktura geometryczna powierzchni, chropowatość.

Streszczenie: W artykule zaprezentowano wyniki badań nad konstytuowaniem stanu naprężeń trwałych w skutek gładkościowego nagniatania. Nieodpowiedni stan naprężeń może powstać podczas sytuacji, w której dążąc do uzyskania coraz wyższej dokładności wymiarowo-kształtowej, mniejszej chropowatości czy też polepszenia nośności powierzchni technolog skłonny jest w zabiegu nagniatania stosować wysokie i bardzo wysokie siły nagniatania F_b. Deformacje plastyczne chropowatości powstałe wskutek nagniatania łatwo można zmierzyć, korzystając ze współczesnych profilometrów. Jednak każdemu zabiegowi nagniatania gładkościowego towarzyszy pewien stan naprężeń, z których część w formie naprężeń trwałych pozostaje w przedmiocie po zakończeniu procesu obróbki. Naprężenia trwałe o zbyt wysokiej wartości w trakcie eksploatacji wyrobów są często źródłem pękania i łuszczenia się fragmentów powierzchni [1, 2]. Jedną z dokładniejszych metod oceny stanu naprężeń trwałych po nagniataniu jest ich modelowanie przy uwzględnieniu własności mechanicznych materiału i wartości parametrów technologicznych stosowanych w trakcie obróbki. O sposobie przygotowania modelu doświadczalnego, jego badaniach i weryfikacji uzyskanych wyników autorzy dokładniej piszą w dalszej części artykułu.

Introduction

One of the factors of cost-effective manufacturing by machining operations is increasingly high performance cutting (HPC). It is particularly well visible in the HPC of items milled using high speed cutting technology for aviation, the automotive industry, or plastics processing. However, the created surface roughness is usually very high and the item requires further machining to reduce roughness.

During the machining of single items such as moulds, die blocks, and dies, technology must guarantee both high efficiency and the required dimension and shape accuracy. In the manufacture of very expensive products, such as moulds and dies, high performance cutting is combined with high performance plastic surface machining (mostly burnishing) [11]. In this case, the production engineer has little margin for error when selecting burnishing force F_b – the basic parameter responsible for machining efficiency, roughness, and the state of stresses [1–10]. Excessive values of burnishing forces contribute to a potentially dangerous state of stresses that, in combination with operating stresses, will lead to rapid loss of the cohesion of the item's surface layer and the core. A negative effect of that phenomenon is flaking and falling off of large fragments of the surface.

Modelling of integrated machining operations (milling and burnishing) allows us to specify kinematic and geometric relations and technological parameters of the cuts combined in one operation. It is also one of the few reliable methods of assessing the values of residual stresses difficult to measure [2]. While modelling an integrated machining process, we can narrow down the range and speed up the selection of desired technological parameters of the two cuts, which combined will not cause potentially dangerous state of residual stresses [12–14].

1. Experimental tests of selecting technological milling and burnishing parameters

We know from studies on integrated profile milling of complex spatial surfaces that milling tools usually leave traces on the machined surface, with prevailing irregularities resulting from the cross feed passes and cutter diameter [1–10, 15] − Figure 1. Inequalities resulting from the feed per revolution are negligibly small. However, burnishing itself is accompanied by plastic phenomena occurring directly in the contact zone of the burnishing tool due to the force of the hard tool with radius R acting on the rough surface of a workpiece. During burnishing, high surface irregularities are reduced due to their plasticizing, followed by filling the irregularity valleys with previously plasticized material. The effect of burnishing is dependent largely on material hardness H and roughness R_{ain} created by cuts preceding burnishing [1–10]. Basic technological parameters of burnishing are burnishing force F_b, feed f_b, and the number of burnishing tool passes np. Of all technological parameters, burnishing speed v_b has the smallest impact on surface roughness [2, 11]. Depending on the hardness of burnished material, one of two methods is used. For soft and plastic materials, slide burnishing is mostly employed [1, 9, 10], in which the coefficient of friction μ between the tip of the burnishing tool and rough surface of the workpiece is a decisive component for the final effect.

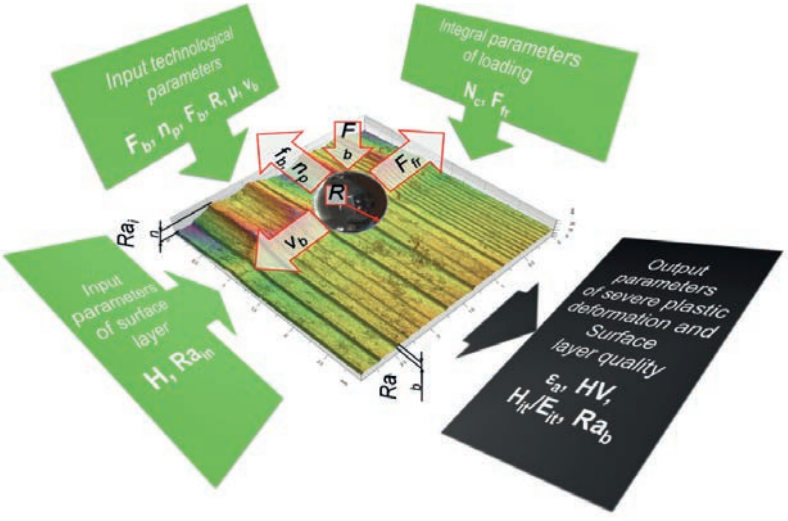

Fig. 1. Input and output parameters of the integrated profile milling with finish burnishing [15]
Source: Authors.

During the burnishing of very hard items, friction forces F_{fr} are minimized by using pressing-roller burnishing, which additionally increases the tool life [2–8]. The kinematics of the burnishing process and technological parameters affect the local load N_c of the surface [6–8] within the workpiece-tool contact area. Besides the final roughness R_{ab}, the process engineer takes into consideration the following output variables of the hybrid machining of a surface: changes in the ratio of surface hardness to stresses in the surface layer H_{it}/E_{it} [2, 12], increase in surface hardness *HV*, and residual stresses σ_a [2]. A certain range of optimal values of the said technological parameters can be identified for burnishing, above which there is no significant improvement of the SGS state [6–8, 14, 15].

Items such as moulds, die blocks, and dies are mostly made of high quality steel alloy, that is why for we have chosen 42CrMo4 steel for tests, which is typical for this type of applications, taking account of the condition after heat treatment up to 35 HRC [14]. During experimental tests, the characteristics of thermally improved material were obtained, i.e. Young's modulus was determined during a tensile test; its value was E = 210 GPa, while Poisson number ν = 0.29, was adopted during the subsequent model tests.

Experimental tests of the machining process were carried out on 100x100x20 mm specimens, profile milled on the machining centre DMG DMU 60MONOBLOCK, with a 15° inclination of the spindle axis – Figure 2a. A torus cutter (WNT R1000G.42.6. type. M16. IK) had six circular cutting inserts with a diameter dp = 10 mm (RD.X1003 MOT – WTN1205). The cutting speed vc = 1 m/min and feed per cutting edge fz = 0.1 mm. The specimens had a regular prismatic shape; therefore, to avoid milling too deep, and due to prior heat treatment, the cutting depth was adopted as ap = 0.5 mm, while the selected cross feed fwm was 0.5 mm.

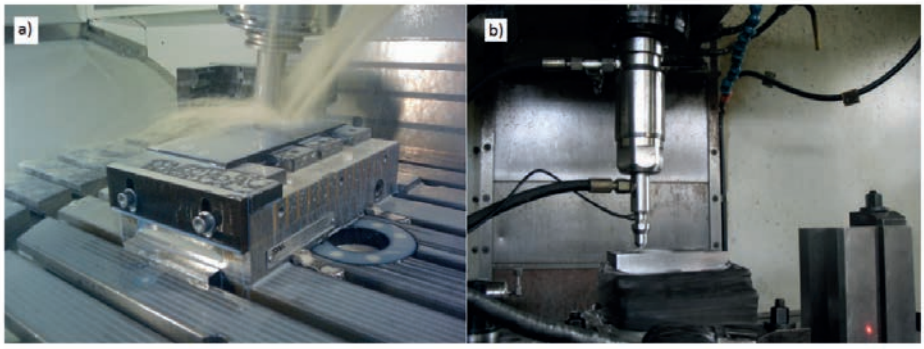

Fig. 2. Preparation of test specimens for tests: a) profile milling with an inclined spindle on the machining centre DMG DMU 60 MONOBLOCK, b) finish burnishing on the three-axial centre MIKRON VCE 500
Source: Own description.

Burnishing was performed on a three-axial milling centre Mikron VCE 500 – Figure 2b. The burnishing tool used was a single-ball hydrostatic tool with a bellows actuator [2, 14], and a tip in the form of a ZrO_2 ball with a diameter db = 10 mm. The burnishing speed vb was 8 m/min, and the cross feed was fwb = 0.12 mm. Burnishing forces F_b applied were, respectively, 250 N, 500 N, and 1000 N. Each of the burnished areas was 11 mm wide. The burnishing balls made of zirconium oxide ZrO_2 (80 HRC) had the same mechanical properties as the properties of steel in the thermally improved condition, i.e. Young's modulus E = 210 GPa, and Poisson number ν = 0.29.

Surfaces of the workpieces after the tests were measured for roughness by a Hommel Etamic T1000 profilographometer with an inductive measuring head TKU300/600 ending with a mapping diamond edge with a 2 µm radius, with a measuring section length of lt = 4.8 mm and consisted of five elementary sections, ln = 0.8 mm. The cut-off used in the tests λc = 0.8 mm in the measuring range of 80µm. Measurement of profile parameters for each surface was repeated five times, setting the mapping edge travel perpendicular to the traces of highest irregularity peaks left by the cutter. The recorded values of typical roughness parameters are shown in Figure 3.

After finish burnishing with a force of 250 N, the parameters Rz and Rt were reduced threefold, compared to the heights of irregularities left after profile milling. The values of the said parameters were similar after burnishing with the forces of 500 N and 1000 N. The reduction of their values was even sevenfold. Yet greater reduction of roughness height parameters was recorded for the most frequently used parameter, Ra (mean arithmetic deviation of profile peaks from the mean line). In this case, for burnishing with a force of 250 N, the reduction of the Ra value was almost sixfold, while the burnishing forces 500 N and 1000 led to an almost tenfold decrease in the Ra value.

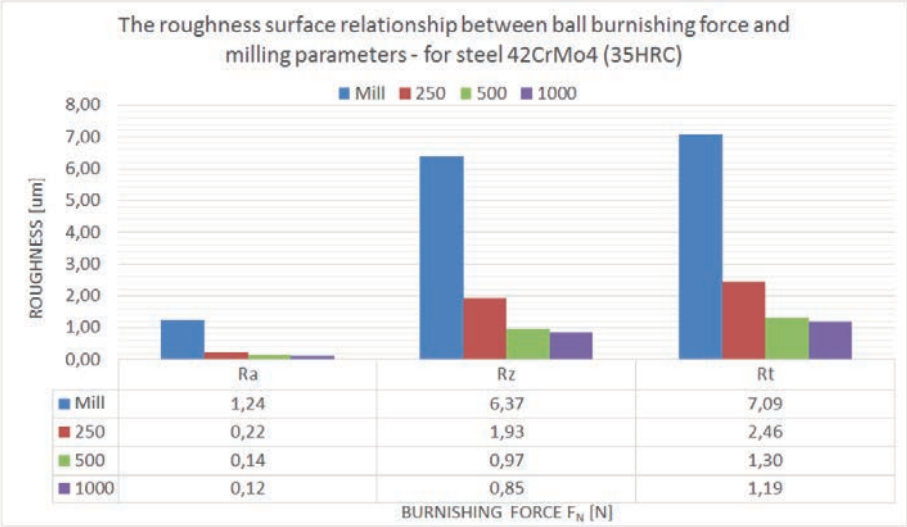

	Ra	Rz	Rt
Mill	1,24	6,37	7,09
250	0,22	1,93	2,46
500	0,14	0,97	1,30
1000	0,12	0,85	1,19

Fig. 3. The roughness parameter values recorded during experimental tests
Source: Authors.

It turns out that, after finish burnishing, very similar results can be obtained using burnishing forces equal to 500 N and 1000 N. Notably, in both cases, stresses will be produced during the machining and subsequent residual stresses in the workpiece surface layer of different, hardly measurable values. The depth and distribution of the stresses in both cases should also be different. The only dependable methods of stress assessment are numerical tests on an experimentally verified model presenting the conformity of vertical displacements of the surface plastic deformation.

2. Computer simulations of hybrid profile milling and finish burnishing of surfaces

For tests of stress values and distribution, we assumed an ideal SGS accounting only for kinematic-geometric conditions of milling with a torus cutter with round inserts, which is similar to experimental studies, and an idealized surface for tests is shown in Figure 4.

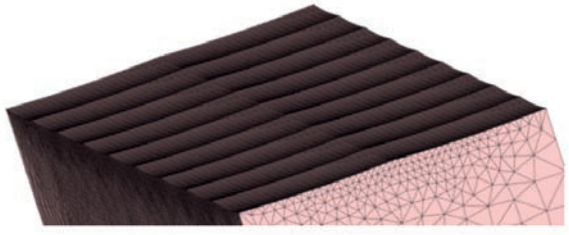

Fig. 4. A view of a computer model representing kinematic-geometric conditions of milling with a torus cutter
Source: Description [14].

Due to hardware limitations, the prepared model specimens had a rectangular prismatic shape with the following dimensions: (width × height × length) 2 × 1 × 4.5 mm. Also, due to the geometrical symmetry of machining, a simplified model was adopted [14]. It is one half of the physical model obtained from a simultaneous intersection of the burnishing ball and the burnished specimen with a plane passing through the centre and perpendicular to the shorter side of the specimen base.

A spherical sector near the contact area of the burnishing ball and the specimen surface is modelled with 245 flat rigid parts and 288 nodes [14]. A section of the prismatic specimen is modelled with 497 516 three-dimensional tetra elements and 91 086 nodes [14]. The prismatic specimen base was fixed, while the nodes located in the pitch plane could move. In the model tests, the same values of burnishing forces F_b as in experimental studies were adopted: 250 N, 500 N, and 1000 N.

The calculations were made by modelling the machining process in a NastranNFX program, using a non-linear static module. Due to the occurrence of contact stresses (the side of a finite element was 0.02 mm), a densified division by finite elements was applied in the area surrounding the contact point between the ball and milled prismatic workpiece surface.

Sensitivity analyses made for the hybrid model of milling and burnishing produced consistent values of plastic deformation and displacements of FEM mesh nodes for finite elements size of only 0.05 mm. Besides, the model permitted the determination of values of the roughness parameter Ra that turned out to agree with the values measured during the experiments [14]. The recorded differences of Ra for the implemented

FEM model did not exceed an acceptable error level. When only the simplified model of the surface, i.e. its kinematic-geometric mapping, the difference in values of parameter Ra between experimental and numerical tests was 18.3%, which is a satisfying result. It should be noted that the observed value of Ra in the experimental measurements of workpieces amounted up to 12% of the average Ra value.

The experimental model, besides being used for the determination of surface plastic deformation values, can be successfully used to define the values of stresses during the burnishing process as well as residual stresses induced in the surface layer of the workpiece. Modelling based on computer simulation becomes practically the only way to assess the state of residual stresses after surface machining of items having spatially complex 3D shape.

3. Tests o f item surface stresses after hybrid machining

The process modelling included the contact and pressing of a burnishing ball into a workpiece surface until a desired value of burnishing force, Fb, was reached. After achieving a preset value of the force, the burnishing ball was being rolled on a surface along a 2 mm section, and then gradually the burnishing force was reduced until the ball left the contact zone. When rolled, the ball rotated by a 23° angle.

A single numerical experiment with calculations by the computer program took about 48 hours. The results included values of surface plastic deformation and associated residual stresses, analysed further in this article. Example values of residual stresses, σy, obtained during the numerical tests are shown in Table 1 and in Figure 5.

Table 1. The mean maximum values of residual stresses determined at a depth using the simulation of a hybrid machining model

Burnishing force	Compressive stresses		Tensile stresses	
Fb [N]	-σy [MPa]	stress depth [mm]	+σy [MPa]	stress depth [mm]
250	-1252	0	123.6	0.48
500	-899	0	97.8	0.9
1000	-408	0	55.2	1.06

Source: Authors.

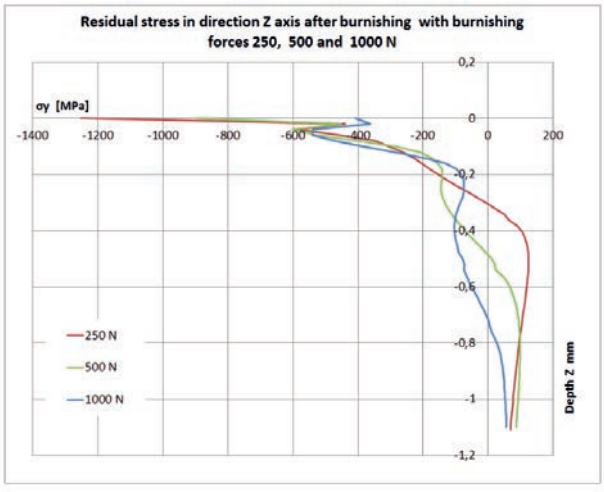

Fig. 5. The stress distribution along the Z axis after burnishing of a rough surface of a 42CrMo4 steel specimen (35 HRC) by a ceramic ball with burnishing forces, respectively, 250 N, 500 N, and 1000 N

Source: Authors.

The tests also covered residual stresses under rough surface after burnishing of a 2 mm section. The test results are illustrated in Figure 6.

During the simulation tests, the obtained curves of stresses in the direction of the burnishing ceramic ball motion were similar. Similar stress distributions were recorded at different depths, depending on the burnishing force applied – Figure 7. The differences (forms and values) of stress distributions on the surface and in its adjacent layers were very large (differences of maximum stress values, σy, exceeded as much as 200%). In the developed simulation model, the variation of stress distribution was acceptable at depths greater than 0.1 mm (three layers of FEM mesh).

Simulation tests on a model are also helpful in selecting the interval of successive cross feed passes f_{wn} of the ball. Depending on the force applied, the scope of plastic deformation and of stress propagation across the basic burnishing direction are different. The passes between subsequent cross feed sections will affect the homogeneity of the surface texture and the homogeneity of stress distribution in surface layers of the workpiece – Figure 8.

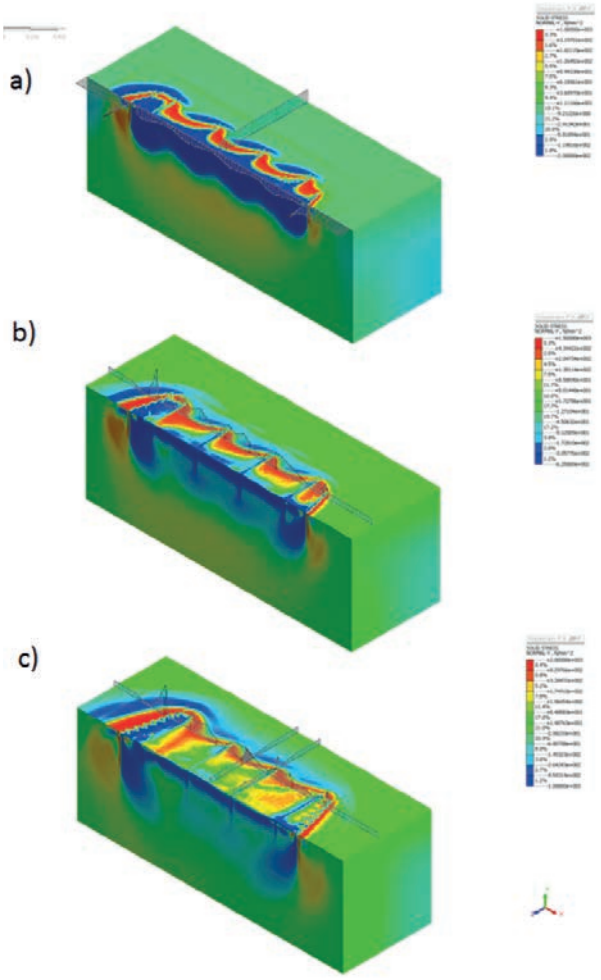

Fig. 6. The residual stress distribution along the Y axis (in the rolling direction of the burnishing ball) after burnishing of a rough surface of a 42CrMo4 steel specimen (35 HRC) with a ceramic ball pressing at a) 250 N, b) 500 N, and c) 1000 N

Source: Authors.

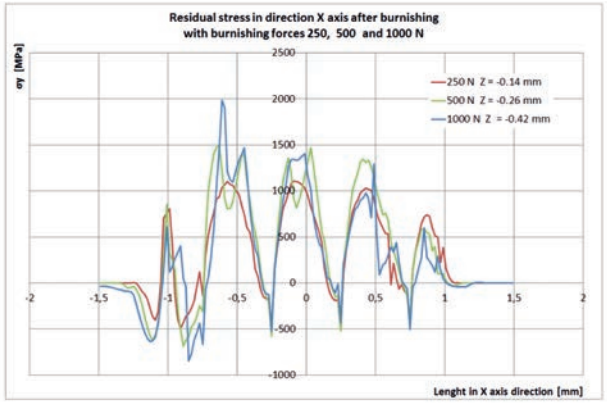

Fig. 7. The residual stress distribution along the X axis (in the direction of burnishing ball rolling) at different depths depending on the burnishing force 250 N, 500 N, and 1000 N

Source: Authors.

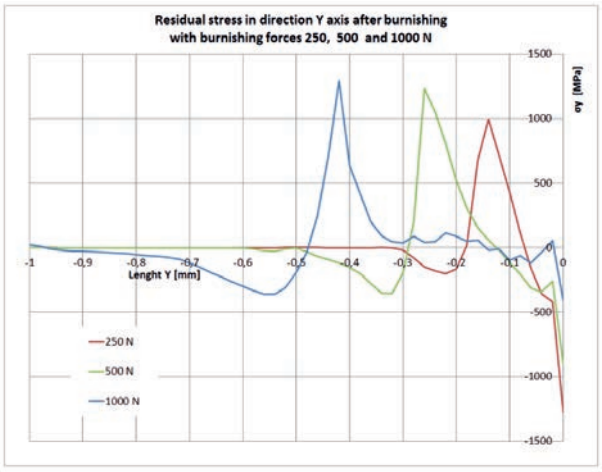

Fig. 8. The residual stress distribution along the y axis (at right angle to the direction of burnishing ball rolling) at different depths depending on the burnishing force 250 N, 500 N, and 1000 N

Source: Authors.

Using a 10mm diameter burnishing ball, we can increase the burnishing process efficiency using large passes between cross feed sections fwn≈0.4 mm, if such machining is done with a force of at least Fb>1000 N. When a smaller burnishing force is used, the passes of the tool should also be reduced (which will reduce the surface area-specific efficiency of burnishing). For burnishing with the forces F_b≈250 N, the cross feed should not exceed f_{wn}<0.15 mm. Besides, the cross feed should not exceed f_{wn}<0.3 mm when forces applied are approx. F_b≈500 N.

A dangerous state of compressive stresses of 42CrMo4 (35 HRC) steel was not exceeded in any of the tests. In some cases of burnishing, a dangerous state of tensile stresses Rm>1046 MPa [2] was observed directly on the surface layer. Such cases were identified in residual stress distributions along the X and Y axes under the surface burnished with a force of 1000 N.

4. Summary and conclusions

The results of numerical studies compared to the results of experimental tests allow us to draw the following conclusions.

The numerical tests were based on an idealized state of the surface geometrical structure after milling, but the adopted simplification has not significantly affected the height SGS parameters. Both numerical and experimental tests have not revealed any essential change in the height parameters of surface roughness after burnishing with forces greater than 500 N.

It seems that the use of a burnishing force of 1000 N and larger may be effective in reducing surface irregularities after milling and in increasing the area-

-specific efficiency of burnishing. However, this significantly increases the potential risk of exceeding a potentially dangerous state of tensile stresses on the surface and right underneath. A simulation model reveals portions of the surface that may become a centre of fatigue wear due to mechanical or thermal use of the workpiece surface.

Points of high concentration of tensile stresses occurring during pressing-roller burnishing may reach 0.5 mm into the core of the material. Recording such subtle changes in the state of stresses at depths for steel workpieces of large volume and spatially complex shape is practically impossible even by using state of the art non-invasive measurement methods based on X-ray diffraction. In such situations, the selection of technological parameters of machining (especially burnishing force) should be supported by numerical tests using a validated model in each case, i.e. model demonstrating the conformity of modelled and recorded real plastic deformations of surface irregularities (which are easy to measure and compare).

Due to hardware and software limitations, preliminary studies comprised modelling of one burnishing pass, whereby the results of surface plastic deformation in the experiment and numerical tests show a certain divergence. The source of observed differences is the propagation of plastic deformation and stresses beyond the zone of direct contact of the workpiece and the burnishing tool. This practically means that subsequent burnishing passes overlap the previously burnished surface, i.e. strengthened in the preceding pass.

In further numerical studies, the adopted area of the varied burnishing forces F_b should be divided at greater density, which will allow accurate identification of the optimal burnishing force F_b. The undertaken numerical tests will be continued. In the future, the experimental model will also be expanded in order to examine the effects of the burnishing of real surfaces after milling (with mesh density range of 0.5–3 μm), in a zone comprising several parallel passes, taking into account the actual state of surface roughness after milling (micro-roughness components).

References

1. Chen C.H., Shiou F.J.: Determination of Optimal Ball-Burnishing Parameters for Plastic injection Moulding Steel, International Journal of Advanced Manufacturing Technology, Vol. 21, issue 3, March 2003, pp. 177-185. DOI: 10.1007/s001700300019.
2. Grochała D., Berczyński S., Grządziel Z.: Stress in the surface layer of objects burnished after milling, International Journal of Advanced Manufacturing Technology, Vol. 72, Issue 9, June 2014, pp. 1655––1663. DOI: 10.1007/s00170-014-5775-x.
3. Gubała R., Grochała D., Olszak W.: Mikrohydrauliczne narzędzie do nagniatania złożonych powierzchni przestrzennych, Mechanik, Nr 1, 2014, pp. 22–23.
4. Kalisz J., Żak K., Grzesik W., Czechowski K.: Characteristics of surface topography after rolling burnishing of EM AW-AlCu4MgSi(A) aluminum alloy, Journal of Machine Engineering, Vol. 15, No. 1, 2015, pp. 71–80.
5. Kwaczyński W., Chmielewski K. Grochała D.: Programowanie frezowania i nagniatania złożonych powierzchni przestrzennych na centrach frezarskich ze sterowaniem wieloosiowym. Współczesne problemy technologii obróbki przez nagniatanie, Tom III – Monografia, pod red. prof. W. Przybylskiego, Gdańsk: Politechnika Gdańska, Wydział Mechaniczny, 2011, pp. 179–191.
6. López de Lacalle L.N., Lamikiz A., Muñoa J., Sánchez J.A.: Quality improvement of ball-end milled sculptured surfaces by ball burnishing, International Journal of Machine Tools & Manufacture, Vol. 45, Issue 15, December 2005, pp. 1659–1668. DOI: 10.1016/j.ijmachtools.2005.03.007.
7. López de Lacalle L.N., Lamikiz A., Sánchez J.A., Arana J.L.: The effect of ball burnishing on heat-treated steel and Inconel 718 milled surfaces. International Journal of Advanced Manufacturing Technology, Vol. 32, Issue 9–10, April 2007, pp. 958-968. DOI: 10.1007/s00170-005-0402-5.
8. Rodríguez A., López de Lacalle L.N., Celaya A., Lamikiz A., Albizuri J.: Surface improvement of shafts by the deep ball-burnishing technique, Surface & Coatings Technology, Vol. 206, 2012, pp. 2817––2824. DOI: 10.1016/j.surfcoat.2011.11.045.
9. Shiou F.J., Chen C.H.: Ultra-precision surface finish of NAK80 mould tool steel using sequential ball burnishing and ball polishing processes, Journal of Materials Processing Technology, Vol. 201, 2008, pp. 554–559, DOI: 10.1016/j.jmatprotec.2007.11.235.
10. Shiou F.J., Chuang C.H.: Precision surface finish of the mold steel PDS5 using an innovative ball burnishing tool embedded with a load cell, Precision Engineering, Vol. 34, Issue 1, January 2010, pp. 7684. DOI: 10.1016/j.precisioneng.2009.03.003.
11. Sosnowski M., Grochała D.: Problemy technologii nagniatania powierzchni przestrzennych złożonych na centrach obróbkowych, Mechanik, Nr 1, 2011, pp. 14–18.
12. Tadic B., Randjelovic S., Todorovic P., Zivkovic J., Kocovic V., Budak I., Vukelic D.: Uising a high-stiffness burnishing tool for increased dimensional and geometrical accuracies of openings, Precision Engineering, Vol. 43, 2016, pp. 335–344. DOI: 10.1016/j.precisioneng.2015.08.014.

13. Żak K., Grzesik W.: Investigation of technological effects of ball burnishing after cryogenic turning of hard steel, Advances in Manufacturing Science and Technology, Vol. 38, nr 1, 2014, pp. 37–52. DOI: 10.2478/amst-2014-0003.
14. Berczyński S., Grochała D., Grządziel Z.: Modelling of surface geometric structure state after integrated milling and finish burnishing, Management Systems in Production Engineering Vol. 26, nr 4, 2017 pp. 131–136, DOI 10.1515/mspe-2017-0020.
15. Bachtiak-Radka E., Dudzińska S., Grochała D., Berczyński S., Olszak W.: The influence of CNC milling and ball burnishing on shaping complex 3D surfaces Surf. Topogr.: Metrol. Prop., Vol. 5, 2017, doi:10.1088/2051-672X/aa539f.